



# Structural restoration of thrusts at the toe of the Nankai Trough accretionary prism off Shikoku Island, Japan: Implications for dewatering processes

**Gregory F. Moore**

*Department of Geology and Geophysics, 1680 East-West Road, University of Hawai'i at Mānoa, Honolulu, Hawaii 96822, USA (gmoore@hawaii.edu)*

**Demian Saffer**

*Department of Geosciences, Pennsylvania State University, 310 Deike Building, University Park, Pennsylvania 16802, USA*

**Melody Studer and Patrizia Costa Pisani**

*Department of Geology and Geophysics, 1680 East-West Road, University of Hawai'i at Mānoa, Honolulu, Hawaii 96822, USA*

[1] A three-dimensional prestack depth-migrated seismic reflection data volume acquired off Shikoku Island, Japan covers the seaward portion of the Nankai Trough accretionary prism. We calculate and interpret total horizontal shortening lengths along three cross-sectional profiles through the volume, incorporating a technique addressing the significant amount of water volume sediments lose during accretion, constrained by porosity values derived from seismic interval velocities. The results reveal a total horizontal shortening of ~40% within sediments of the first three thrust sheets in the wedge. This indicates that structural restorations applied to water-saturated young sediments, or other domains displaying large tectonic-induced porosity changes (e.g., accretionary prisms, subaerial and submarine fold and thrust belts), must account for the substantial amount of distributed compactive strain that affects the sediment during the initial stages of accretion. Our analysis of the porosity reduction also allows an estimate of dewatering rates across the outer accretionary wedge. We find that porosity loss and associated dewatering decrease with distance landward from the trench and correspond to a progressively decreasing contribution of diffuse compactive strain to the total shortening. We compute a dewatering rate of 10.5 km<sup>3</sup>/Ma (per km along strike) over the outer ~7 km of the accretionary wedge. This relatively high rate of dewatering when compared to other well-studied subduction systems probably reflects the large thickness of accreted sediment and high sediment permeability that allows efficient consolidation. These results highlight the importance of considering distributed compactive strain in structural restorations for any setting where deformation occurs in sediments.

**Components:** 7300 words, 9 figures, 1 table.

**Keywords:** Nankai Trough; structural restoration; dewatering.

**Index Terms:** 3060 Marine Geology and Geophysics: Subduction zone processes (1031, 3613, 8170, 8413); 3025 Marine Geology and Geophysics: Marine seismics (0935, 7294).

**Received** 1 December 2010; **Revised** 18 March 2011; **Accepted** 28 March 2011; **Published** 11 May 2011.

Moore, G. F., D. Saffer, M. Studer, and P. Costa Pisani (2011), Structural restoration of thrusts at the toe of the Nankai Trough accretionary prism off Shikoku Island, Japan: Implications for dewatering processes, *Geochem. Geophys. Geosyst.*, 12, Q0AD12, doi:10.1029/2010GC003453.

**Theme:** Mechanics, Deformation, and Hydrologic Processes at Subduction Complexes,  
With Emphasis on the Nankai Trough Seismogenic Zone Experiment  
(NanTroSEIZE) Drilling Transect

**Guest Editors:** D. Saffer, H. Tobin, P. Henry, and F. Chester

## 1. Introduction

[2] Accretionary prisms are primary structural components of convergent margins with thick sediment covers, such as the Aleutians, Barbados, Nankai Trough and Sunda [e.g., von Huene and Klaeschen, 1999; Moore et al., 1998, 1990; Kopp and Kukowski, 2003]. During subduction, sediment is off scraped from the oceanic plate and forms an accretionary prism along the margin. Earthquake rupture along the main basal plate boundary fault, or décollement, beneath the wedge poses a large seismic and tsunami threat to numerous coastal regions worldwide. Significant progress in understanding subduction zone processes and the characterization of convergent margins during the last three decades has been achieved through seismic investigation [e.g., Westbrook et al., 1988; Moore et al., 1990; Shipley et al., 1994; Park et al., 2000, 2002] and drilling into accretionary prisms [e.g., Taira et al., 1991; Westbrook et al., 1994; Shipley et al., 1995; Moore et al., 1998, 2001], as well as through laboratory experiments and theoretical studies [e.g., Bekins and Sreaton, 2007; Saffer and Bekins, 2002; Sreaton et al., 1990]. However, understanding the mechanics, deformational response, and associated dewatering of sediments during the initial stages of accretion is limited by a lack of detailed and quantitative information about deformation at the toe of the prism.

[3] Removing accumulated strain in the wedge through structural restoration methods is one approach to obtain horizontal shortening estimates, and thus to define the response of sedimentary facies to deformation during accretion. Our understanding of mechanical conditions within and beneath the wedge can be improved by quantifying the amount of horizontal shortening through structural restoration, and in particular by defining the component of shortening accommodated by ductile strain that reflects consolidation and porosity loss. Estimates of this compactive volume loss also provide constraints on the distribution of porosity reduction and dewatering across the outer accretionary complex. Although several studies have quantitatively estimated dewatering rates using numerical models [e.g., Bekins and Dreiss, 1992;

Le Pichon et al., 1990] or global compilations of porosity data [Bray and Karig, 1985], water loss due to progressive compaction has generally not been rigorously quantified from data, mainly owing to lack of sufficient constraints on porosity distribution at individual margins.

[4] Here, we examine a three-dimensional (3-D) seismic reflection volume acquired along the Muroto transect south of Shikoku Island in 1999 [Moore et al., 1999; Bangs et al., 2004; Gulick et al., 2004] (Figure 1). The Nankai Trough region is a focus for investigation partly because it has a 1300 year historical record of recurring great earthquakes, including the 1944 Tonankai ( $M_w$  8.1) and the 1946 Nankaido ( $M_w$  8.2) earthquakes [Ando, 1975]. Located off the southeast coast of Japan (Figure 1), the Nankai Trough has been extensively studied in recent years during Ocean Drilling Program (ODP) Legs 131,190, and 196 [Taira et al., 1991; Moore et al., 2001; Mikada et al., 2002]. Additionally, the region has been imaged by a series of seismic reflection and refraction surveys [Aoki et al., 1982; Leggett et al., 1985; Aoki et al., 1986; Moore et al., 1990, 1991, 1999; Park et al., 1999, 2000; Kodaira et al., 2000]. A map view of the bathymetry of outer wedge study area, in addition to the orientation and location of specific profiles utilized in this study, are shown in Figure 2. The 3-D survey, conducted with a single streamer on the R/V *Maurice Ewing*, consisted of 81 shot lines, each 80 km long. The lines are 100 m apart, so the width of the survey is 8 km. The seismic source was a tuned array of 14 air guns with a volume of 70 L (4273 in<sup>3</sup>). The receiver array was 6000 m long with 240 channels at 25 m spacing. Data processing consisted of binning to yield 181 inlines with 50 m crossline spacing and 25 m inline spacing, trace editing, trace interpolation and filtering (5-8-65-80 Hz) followed by 3-D prestack depth migration (PSDM) constrained to match depth at the ODP drill sites [Costa Pisani et al., 2005].

[5] The primary goal of this paper is to estimate total horizontal shortening along the outer wedge toe of the Muroto transect by using 2-D structural restoration, and quantify the contribution of ductile processes (consolidation and porosity loss) to the total shortening. The restorations focus on a rela-

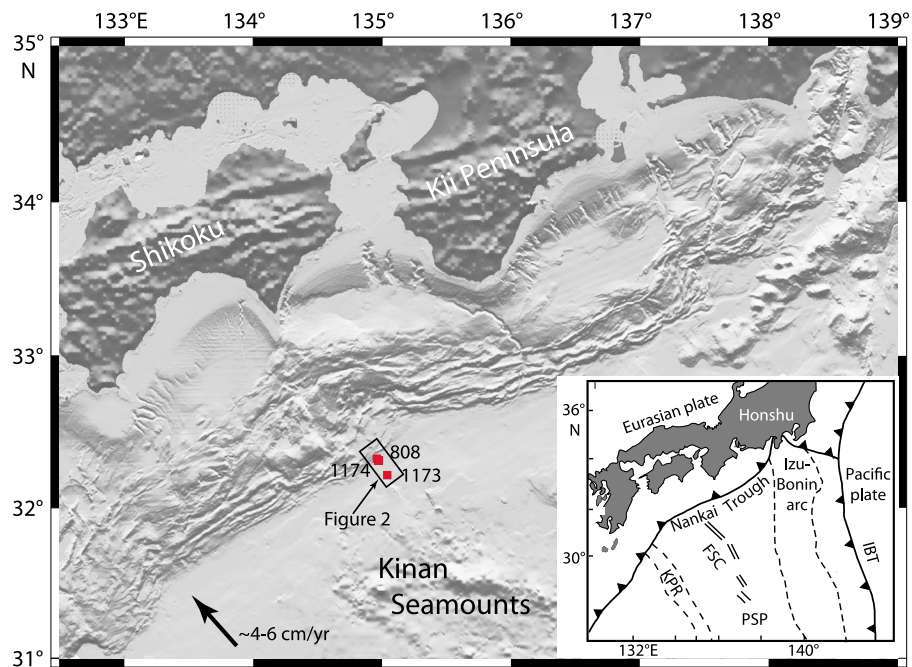


**Figure 1.** Shaded relief map of the Nankai Trough and northern Shikoku Basin, with locations of ODP drill sites (808, 1173, and 1174) used in this study. Arrow indicates subduction direction of Philippine Sea plate beneath Japan. Location of Figure 2 is shown in the box. Inset is a regional tectonic map showing setting of the Nankai Trough study area. KPR, Kyushu-Palau Ridge; FSC, fossil spreading center; PSP, Philippine Sea plate; IBT, Izu-Bonin Trench.

tively small study area comprising the seaward most part of the 3-D volume, in order to provide a detailed view of processes occurring during initial frontal accretion, which are perhaps overlooked in studies encompassing the entire accretionary prism. Finally, high-quality velocity and porosity information derived from the 3-D volume allow detailed quantification of dewatering rates in the outer

wedge, as well as comparisons to other accretionary prisms.

## 2. Geologic and Tectonic Setting

[6] The Philippine Sea plate subducts beneath the Eurasian plate along southwestern Japan at the Nankai Trough. Off the coast of Shikoku Island,

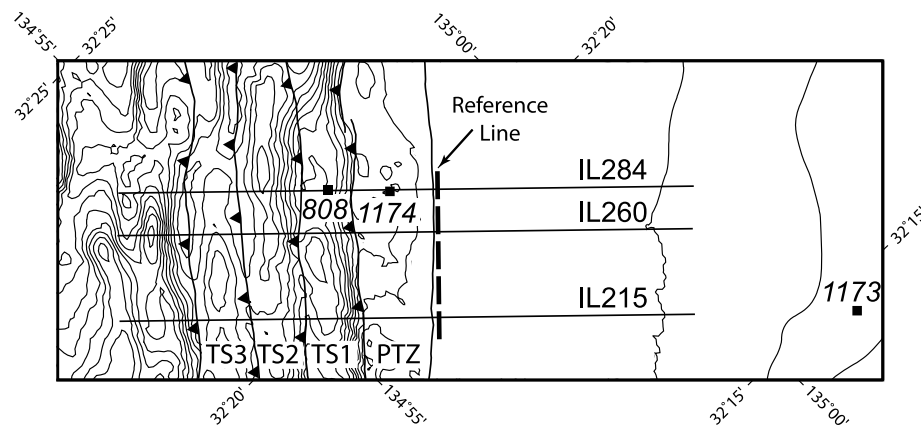


**Figure 2.** Map view of the bathymetry in the Muroto 3-D seismic survey, showing the locations of the restored 3-D seismic inlines (IL215, IL260, and IL284), along with major thrust faults and thrust packages (PTZ, protothrust zone; TS, thrust sheet). The reference location used in the structural restoration is along crossline 685. ODP sites are shown as solid squares.

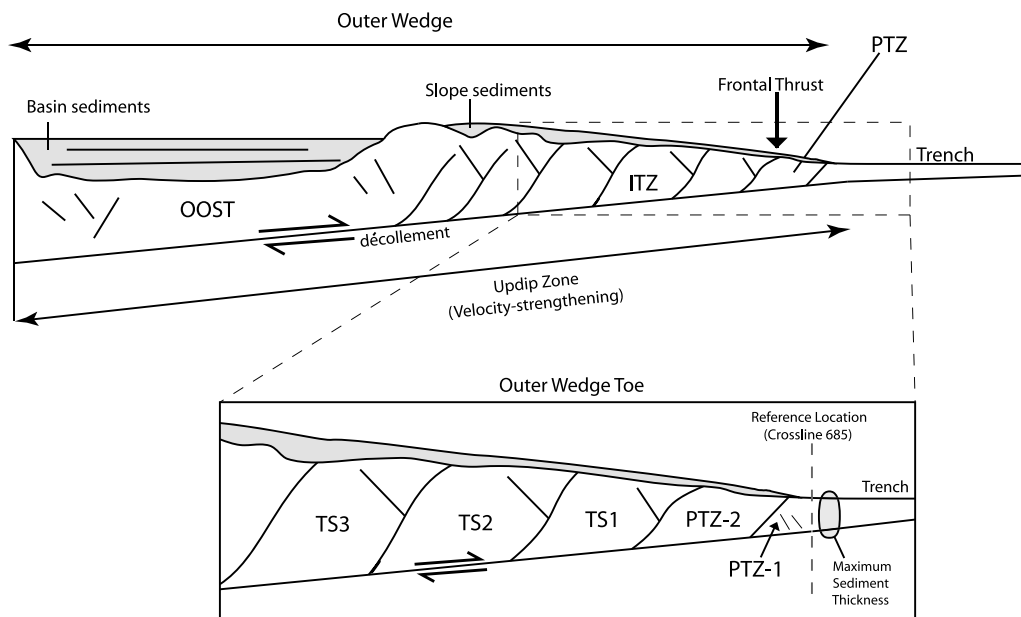


**Figure 3.** Schematic profile of the Nankai accretionary prism showing the location of the outer wedge and different tectonic zones. The outer wedge toe region, comprising the first, second, and third thrust sheets (TS1, TS2, and TS3, respectively) and protothrust region (PTZ-1 and PTZ-2), used in our structural restoration are shown in the magnified subset. Seaward of the reference location, tectonically undeformed trench sediments reach a maximum sediment thickness. Landward of the reference site (in the PTZ-2 region), small-scale backthrusts begin to thicken and deform the sediment pile.

convergence is to the NW at  $\sim 4\text{--}6$  cm/yr [Seno *et al.*, 1993; Miyazaki and Heki, 2001]. A décollement forms within the thick hemipelagic sediments on the subducting Philippine Sea plate, separating a lower section that is subducted beneath the accretionary wedge from an upper section that is accreted to the toe of the margin, thus forming a wide frontal accretionary prism. The subaerial Shimanto Belt located on Shikoku Island has been interpreted as evidence that accretion began in the late Cretaceous [Taira *et al.*, 1988; Ohmori *et al.*, 1997]. However, accretion was most likely not continuous throughout the history of the prism, or the wedge would be much larger than it is today [Taira, 2001]. The current period of accretion, estimated from drill core data, is thought to have begun during the Pliocene [Moore *et al.*, 2001].

[7] Previous interpretations of seismic reflection data in the region divide the outer accretionary prism into three distinct tectonic zones [Moore *et al.*, 1999; Gulick *et al.*, 2004]: (1) the protothrust zone (PTZ), (2) an imbricate thrust zone (ITZ), and (3) a region of out-of-sequence thrusting (OOST) (Figure 3). The PTZ is bounded by the deformation front at its seaward edge and by the frontal thrust at its landward edge. The ITZ begins at the frontal

thrust and ends  $\sim 30$  km landward, and is characterized by numerous conjugate thrust faults. The OOST zone extends landward from the ITZ and is bounded by a large seafloor ridge. The bathymetric slope of the frontal ITZ region is  $1\text{--}1.5^\circ$ , and increases to  $\sim 5\text{--}6^\circ$  landward of the first OOST [Moore *et al.*, 1999; Kimura *et al.*, 2007]. In this study, we focus on the outer wedge toe of the Nankai prism, including the trench, PTZ, and frontal portion of the ITZ (Figure 3).

[8] Knowledge of depositional and deformational styles of the accreted sediments provides several constraints in constructing restorations. A cross section of the prism toe along line 284 (Figure 4) shows the interpretation and stratigraphic relationship between the Shikoku Basin hemipelagic facies and turbidite sequences (see also Shaw *et al.* [2005] for details of interpretation of this region). Our seismic interpretation is based on geologic information from drill Sites 808 and 1174 [Taira *et al.*, 1991; Moore *et al.*, 2001]; both sites penetrate the décollement and provide constraints on lithostratigraphy, ages, and physical properties (including porosity and acoustic velocity) for the accreted wedge and underthrust sediments. The basal section is composed of hemipelagic sediments which

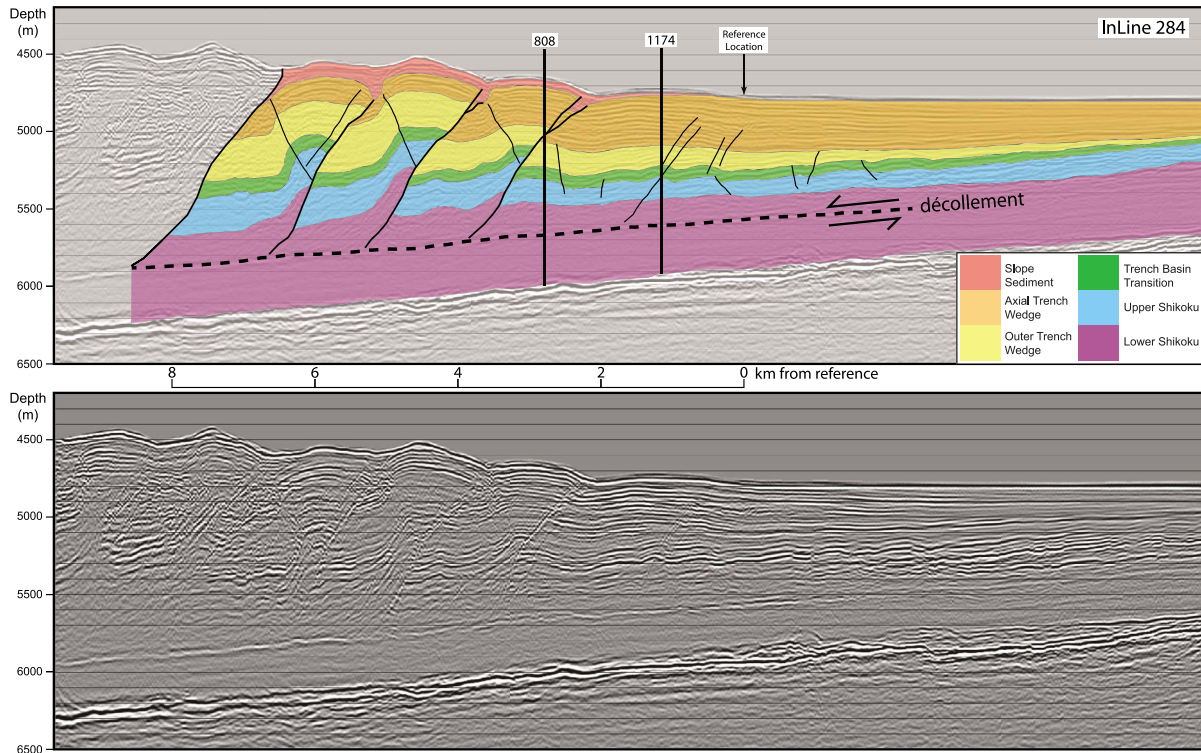


**Figure 4.** Seismic cross-section profile and interpretation of inline 284 within the Muroto transect. (top) The interpretation of major faults and sediment facies used for restorations and (bottom) the uninterpreted line. Drill sites 808 and 1174 are shown in their respective locations and are used to constrain the interpretation. The stratigraphic column defines the individual sediment facies. The slope deposits (pink) are composed of slumped sediment related to movement along imbricate thrust faults, as described in the text. The décollement (dashed line) forms within the Lower Shikoku Basin facies and separates the accreted material (above) from the subducted material (below).

were deposited in the Shikoku Basin over the ~15 Ma since its formation, whereas the trench sediments consist of rapidly deposited Quaternary turbidites [Taira *et al.*, 1991]. Trench sediment thickness reaches a maximum at the landward margin of the trench, thinning and onlapping the hemipelagic sediments in the seaward direction. When accreted to the margin, trench sediments and the underlying Shikoku Basin sediments thicken arcward through a combination of diffuse and brittle deformational processes [e.g., Morgan and Karig, 1995]. The apparent loss of the axial trench wedge facies (e.g., Figure 4), comprising unconsolidated muddy sand, silt turbidites, and hemipelagic mud, from the seaward portion of each thrust sheet is primarily attributed to slumping during thrust movement. Increased slip on faults in progressively landward thrust sheets causes a larger seafloor relief, providing a mechanism for sediment slumping. These slump deposits thicken in the landward direction due to the landward increase in

fault slip and greater time for their accumulation (Figure 4).

### 3. Structural Restoration Methods

[9] Structural restoration involves interpreting geologic structures in order to reconstruct the evolution of rock geometries and deformation. Cross-section restoration was first applied to subaerial thrust belts, using the assumption of constant bed length and thickness [Bally *et al.*, 1966; Dahlstrom, 1969]. The assumption of constant bed length implies that slip along bedding planes is the dominant deformation mechanism [Davison, 1986; Suppe, 1983; Xiao and Suppe, 1993]. The lateral stressing and active deformation of soft sediments in accretionary prisms complicates the traditional bed length or area balancing assumptions [Woodward *et al.*, 1985] and, therefore, requires careful evaluation. First, sedimentation and deformation are occurring

simultaneously in an accretionary prism, so the basic framework is different from a classic thrust belt where the deforming rocks are very old and strongly consolidated at the time of deformation. Second, and perhaps more importantly, because the deforming sedimentary section is very young and is still compacting, strain is accommodated partly through decreasing porosity [e.g., *Morgan and Karig, 1995; Henry et al., 2003*]. Although decreased porosity of the trench fill and underlying pelagic sediment sections with depth is explained by uniaxial consolidation [*Taira et al., 1991*], arcward reduction in porosity attributed to tectonic strains [e.g., *Bray and Karig, 1985*] substantially contributes to shortening and convergence estimates [*Morgan and Karig, 1995; Henry et al., 2003*].

[10] We used the PSDM interval velocity model calculated by *Costa Pisani et al. [2005]* for the Muroto transect 3-D volume to estimate porosity using a relationship defined for the Nankai Trough prism sediments by *Hyndman et al. [1993]*. Given the uncertainties in the velocity estimates ( $\pm 5\%$ ), *Tobin and Saffer [2009]*, who used these same PSDM velocities, report that the propagated uncertainty in porosity calculated from the PSDM velocities is  $< \pm \sim 10\%$ , which we believe to be adequate for our restorations. Porosity values derived from the interval velocities are also tied to shipboard porosity measurements at ODP Sites 1174 and 808 (see *Tobin and Saffer [2009]* for details of this technique). We then transformed the porosities into cross-section area ratios using a technique similar to that of *Morgan and Karig [1995]* and assuming conservation of solid (sediment grain) volume:

$$\frac{A_o}{A} = \frac{(1 - \gamma)}{(1 - \gamma_o)}, \quad (1)$$

where  $\gamma$  represents the final average porosity in each deformed state, and  $\gamma_o$  is the initial porosity at an undeformed reference location. The area ratio,  $\frac{A_o}{A}$  describes the cross-sectional area change between the deformed and undeformed configurations caused by porosity loss. We interpreted and restored a series of three cross sections (lines 215, 260, and 284) using the structural restoration software package LithoTect™. We restricted our reconstructions to the southwest part of the 3-D survey area because of complications due to the frontal thrust stepping landward to a new thrust in the northeast part of the survey area (Figure 2)

[*Gulick et al., 2004*]. Restorations span the outer accretionary wedge including the first, second and third thrust sheets (TS1, TS2, and TS3, respectively) and the protothrust zone (PTZ-1 and PTZ-2) (Figure 3).

[11] In order to determine the amount of strain caused by lateral compaction and porosity loss, we must first define the initial porosity of each layer at an undeformed reference site. We choose a reference site along crossline 685, at a location slightly seaward of the PTZ, where the trench sediments reach a maximum thickness, and where we assume there is negligible lateral compaction [*Morgan et al., 2007*] (Figures 2–3). We obtain our reference undeformed porosity value ( $\gamma_o$ ) by transforming the velocities at this location into average porosities for each stratigraphic unit shown in Figure 4. By applying *Hyndman et al.'s [1993]* velocity-porosity relationship for marine mudstones to the entire data set, we calculate average porosities ( $\gamma$ ) in each individual deformed thrust sheet. Assuming that the initial thickness of each unit was uniform, the undeformed and deformed porosity values are used in equation (1) to calculate the area correction applied in our structural restoration. We believe that the assumption of uniform initial unit thickness is valid over the limited lateral extent of the individual thrust sheets (compare Figure 4).

[12] PSDM porosities calculated in the deformed landward regions are restored to the average initial porosity of each layer at the reference location, using equation (1). Porosities measured from core samples at ODP Sites 808 and 1173 [*Taira et al., 1991; Sreaton et al., 2002*] provided a control section within the prism, and porosity estimates further landward in the wedge are calculated through the PSDM interval velocity data. The porosities extrapolated landward and at depth within the prism have some uncertainties away from the drill holes; however, use of the 3-D velocity data for the extrapolation significantly improves upon previous studies [*Morgan and Karig, 1995*].

[13] The first step of the restoration, area balancing, consists of unslipping offsets on the major faults (Figure 5), which yields estimates of shortening by fault slip and constant-volume strains. These strains could be achieved through localized slip on subseismic faults as well as distributed microscopic flow. Removal of this horizontal shortening ( $S_{fs}$ ), calculated through a length-scale ratio measured along the décollement (Figure 5), extends the

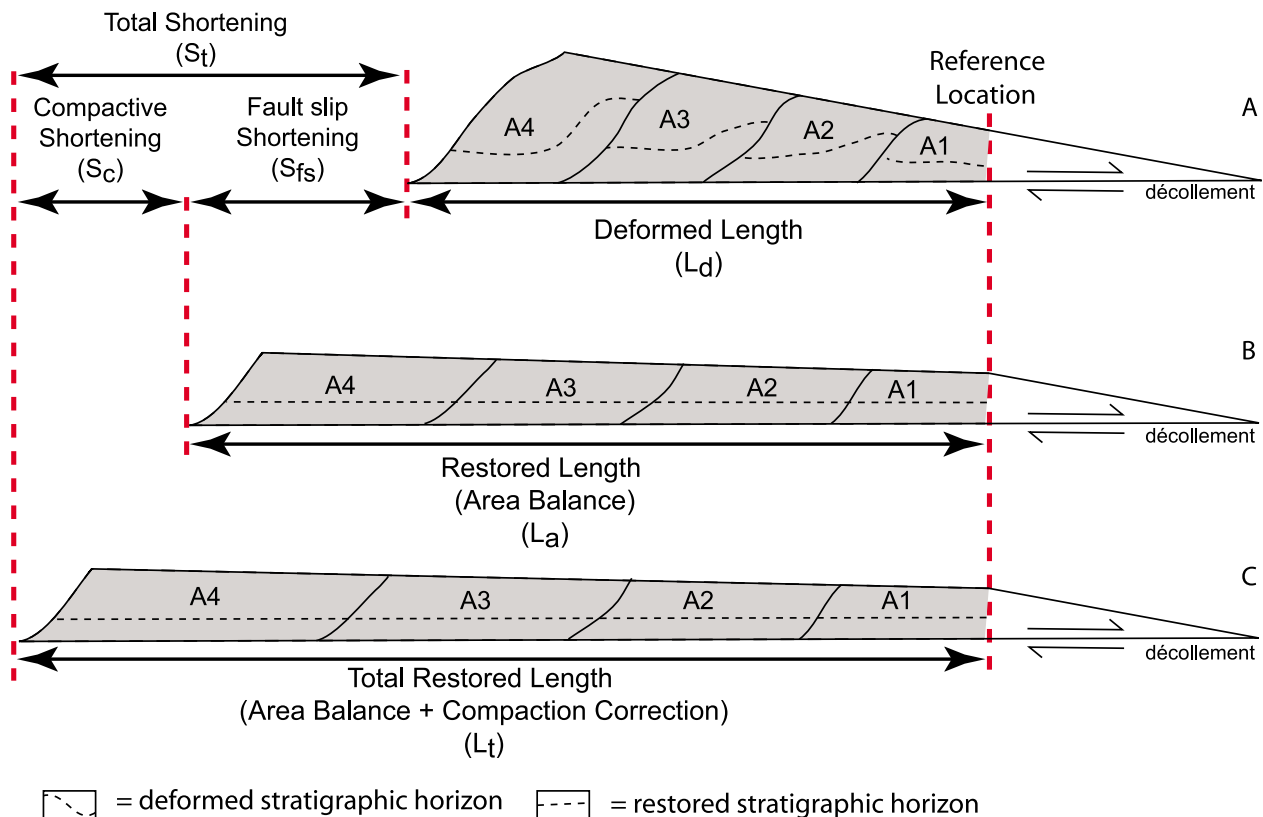


**Figure 5.** Schematic illustration of the horizontal shortening calculation used in this study. Lengths are measured from the reference location (crossline 685) to the end of the third thrust sheet along the décollement. Note that the schematic areas (shaded zones) have been rotated to make the décollement horizontal. An area balance restoration corrects for fault slip along the main thrust faults, but maintains the same area within the thrust sheets (A1, A2, A3, and A4). Application of a compaction correction to the area balanced section yields a larger restored cross-sectional area and restored length (A1 + porosity area).

original deformed length ( $L_d$ ) to a partially restored length ( $L_a$ ) in which the area within each restored thrust sheet remains the same as it was in its deformed state. The restored section is also bed length balanced along the stratigraphic horizons. This structural restoration only accounts for the slip along the main thrust faults and distributed constant-volume strains, however, so it is not realistic for compacting soft sediments in submarine settings, which undergo significant volume loss caused by dewatering during initial accretion. The final step in the restoration is to apply a correction to account for this layer-parallel compaction. The correction is manifest as a uniaxial horizontal lengthening ( $S_c$ ) to produce the total restored lengths ( $L_t$ ).

[14] This restoration results in a significantly larger original cross-sectional area and therefore results in an overall larger horizontal shortening. The restoration method allows us to estimate the relative contributions of slip on thrust faults and distributed sediment porosity loss to the total shortening, and

also provides constraints on the distribution of dewatering.

## 4. Results and Discussion

### 4.1. Horizontal Shortening

[15] Comparisons of the deformed and undeformed configurations of the three cross sections along the Muroto transect provide estimates of along strike variations in horizontal shortening at the prism toe (Table 1 and Figure 6). The difference in total length between the porosity-corrected ( $L_t$ ) and deformed states ( $L_d$ ) indicates a total horizontal shortening (Table 1) range of 5.37–6.38 km or horizontal strains of 39–43% across the outer wedge. Restoring the displaced strata based strictly on area and bed length balancing techniques recovers only 1.3–2.0 km or ~24–35% of the total shortening, implying that the majority of shortening is accommodated by porosity reduction.

**Table 1.** Horizontal Shortening Estimates Along Three Seismic Inlines Across the Muroto Transect

Region	$L_d$ Deformed Length (km)	$S_{fs}$ Fault Slip Shortening (km)	$S_c$ Compactive Shortening (km)	$S_t$ Total Shortening (km)	$\frac{S_c}{S_t}$ (%)	$L_a$ Area Balance Restored Length (km)	$L_t$ Total Restored Length (km)	$S_{fs}$ Fault Slip Shortening (%)	$S_c$ Compactive Shortening (%)	$S_t$ Total Shortening (%)
<i>Inline 215</i>										
Total	8.44	1.98	3.68	5.66	65	10.42	14.1	14.0	26.1	40.1
TS3	1.84	1.10	1.69	2.79	61	2.94	4.63	23.8	36.5	60.3
TS2	1.36	0.44	1.00	1.44	69	1.80	2.80	15.7	35.7	51.4
TS1	1.74	0.36	0.56	0.92	61	2.10	2.66	13.5	21.1	34.6
PTZ-2	1.91	0.07	0.25	0.32	78	1.98	2.23	3.1	11.2	14.3
PTZ-1	1.59	0.01	0.18	0.19	95	1.60	1.78	0.6	10.1	10.7
<i>Inline 260</i>										
Total	8.48	1.55	4.83	6.38	76	10.03	14.86	10.4	32.5	42.9
TS3	1.58	0.42	1.40	1.82	77	2.00	3.40	12.4	41.2	53.5
TS2	1.48	0.62	0.99	1.61	62	2.10	3.09	20.1	32.0	52.1
TS1	1.70	0.28	1.15	1.43	80	1.98	3.13	8.9	36.7	45.7
PTZ-2	2.19	0.18	0.98	1.16	85	2.37	3.35	5.4	29.3	34.6
PTZ-1	1.53	0.05	0.31	0.36	86	1.58	1.89	2.6	16.4	19.0
<i>Inline 284</i>										
Total	8.36	1.31	4.06	5.37	76	9.67	13.73	9.5	29.6	39.1
TS3	1.86	0.52	1.05	1.57	67	2.38	3.43	15.2	30.6	45.8
TS2	1.27	0.34	1.03	1.37	75	1.61	2.64	12.9	39.0	51.9
TS1	1.44	0.25	0.87	1.12	78	1.69	2.56	9.8	34.0	43.8
PTZ-2	2.10	0.19	0.74	0.93	80	2.29	3.03	6.3	24.4	30.7
PTZ-1	1.69	0.01	0.37	0.38	97	1.70	2.07	0.5	17.9	18.4

This indicates that structural restorations applied to contractionally deformed, unconsolidated sediments must account for substantial dewatering and consolidation during the initial stages of deformation. We estimate that the total horizontal shortening results have an error of about  $\pm 10\%$  based on the uncertainty in computed porosity. The error is constrained by inserting a range of initial and deformed porosities into equation (1) based on a weighted average estimate per stratigraphic unit.

[16] The length difference between total horizontal shortening ( $L_t$ ), which includes both a porosity loss correction and slip along faults, and a restoration that only accounts for fault slip ( $L_a$ ) allows us to determine the proportion of total shortening that is specifically attributed to the diffuse compactive strain (i.e., porosity loss) within the sediments. This proportion varies along the margin, ranging from 65% at line 215 in the SW to 76% estimated at lines 260 and 284. The proportion of shortening accommodated by compactive strain also decreases systematically with distance landward, from 86 to 97% in PTZ-1, to values as low as 60–77% in TS2 and 3 (Figure 7 and Table 1). This corresponds to a decrease in the average porosity within the accretionary wedge from  $\sim 50\%$  to  $\sim 32\%$ . For all of the

individual thrust slices, this proportion is  $>60\%$ , and generally  $>70\%$ .

[17] Previous studies in this region estimated a minimum total shortening of 31% within the first two thrust sheets at ODP Site 808 [Morgan and Karig, 1995]. Of this, the component attributed to compactive strain (about 68% in the vicinity of drill Site 808) was determined by the ratio between the length of the décollement after the complete restoration and the length of the décollement after the restoration of only the folded and displaced strata (similar to the area balancing restoration in Table 1) [Morgan and Karig, 1995]. In comparison, along Line 284, we calculate 48% shortening within TS-1 and -2, with 76% of the total attributed to compactive strain. Two possible explanations for the slightly lower values reported by Morgan and Karig [1995] include (1) the assumption of no volume change along the base of the prism, which provides a minimum limiting solution, and (2) sparse velocity logs and 2-D seismic data used in the study limit the resolution of porosity distribution. For our purposes, the PSDM velocity-porosity transforms used in this study provided increased precision in applying a porosity correction. Henry et al. [2003] estimate 10–15% strain associated

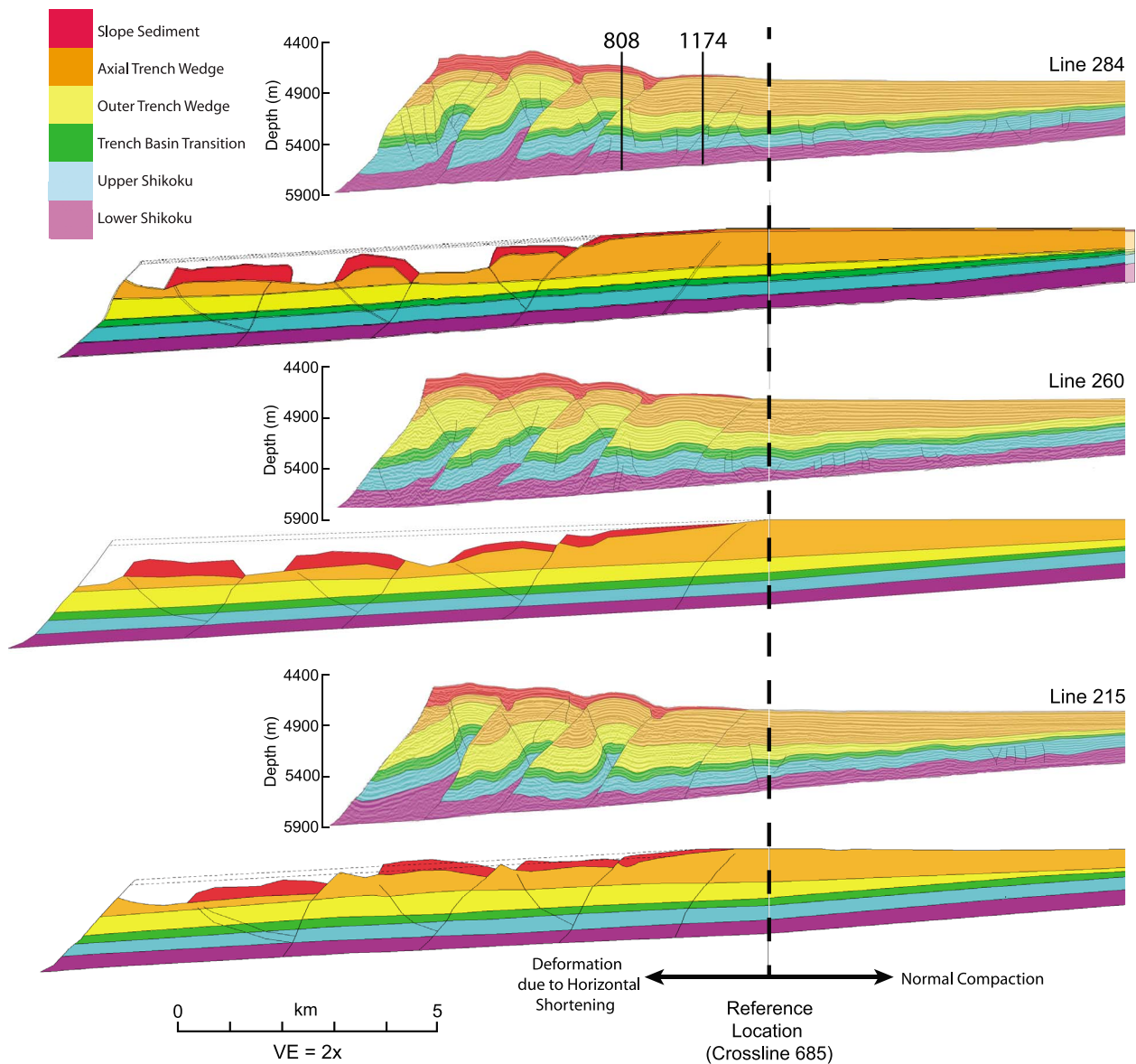


**Figure 6.** Interpreted PSDM profiles and corresponding porosity-corrected structural restorations across the Muroto transect region of the Nankai Trough shown at 2:1 vertical exaggeration. Main stratigraphic facies correlated within the protothrust zone, first, second, and third thrust sheets are shown in their defined colors. Trench fill sediments are orange and yellow, facies transition is green, and Shikoku Basin sediments are blue and purple. The locations of ODP Hole 808 and 1174 are also indicated along line 284. Restored sediment thicknesses represent the compaction state found at the reference location (crossline 685). The apparent loss of the outer trench wedge facies in the thrust sheets is attributed to submarine erosion. Restored estimates of the eroded surface and the slope sediment facies are shown with dashed lines.

with porosity loss at ODP Site 1174 and infer only minor shortening due to slip along faults. Our calculations for Line 284 in PTZ-1 and -2 similarly show only minor fault-related shortening (~4%), and somewhat larger (22%) total strain from compactive shortening. We consider this difference to be remarkably small, given the significant difference in the two techniques.

## 4.2. Porosity Loss and Dewatering Rates

[18] The seismically derived porosity distribution for the outer accretionary wedge allows estimation of both the porosity loss within each stratigraphic unit, and the rate of dewatering of the accreted strata as a function of distance from the trench. Here, we report porosity reduction and dewatering

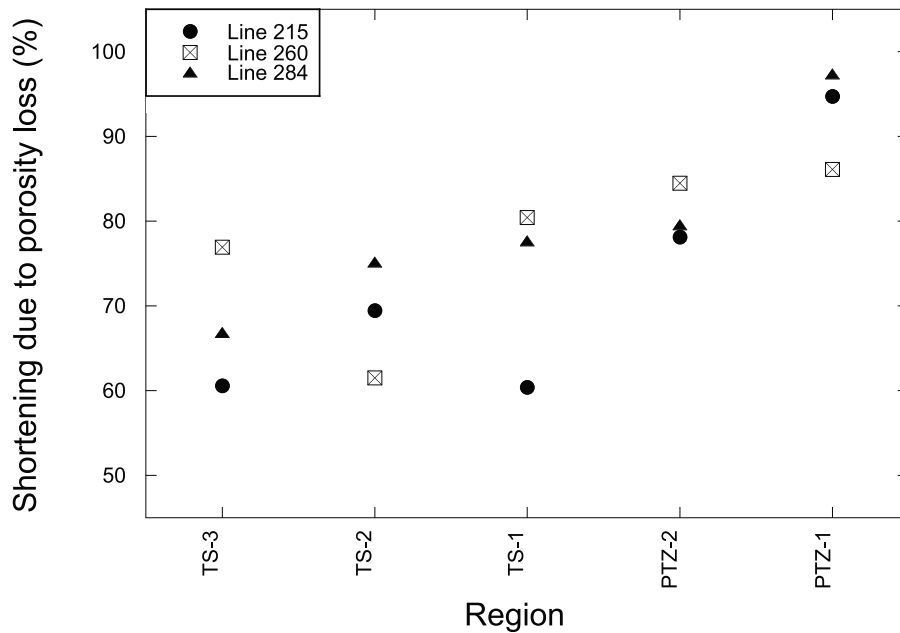


**Figure 7.** Proportion of shortening accommodated by dewatering/compactive porosity loss as a function of structural position relative to the trench.

rates using line 284 as an example. The average porosity of the accreted strata is reduced from ~50% at the trench reference location (CDP 685), to ~32% by TS-3 (Figure 8), with most of the reduction (from ~50% to 35%) occurring in the outer ~4 km between the trench and TS-1. The trench sediments and hemipelagic Shikoku Basin facies exhibit similar patterns of porosity loss with progressive thrust deformation (Figure 8). The rate of porosity reduction in the outermost ~2–4 km of the wedge is higher than that for the rapidly buried (and presumably lower permeability) underthrust sediment section (Figure 8b), but the two are comparable arcward of TS-1. The pattern of decreased porosity loss with distance arcward mirrors the pattern of decreasing diffuse compactive shortening (see Figure 7) and is consistent with the strain hardening behavior of sediment during consolidation.

[19] Using the porosity distribution (Figure 8a), we calculate dewatering rates within each zone by assuming (1) conservation of solid mass (or in this case, solid area) and (2) that the initial thickness of each unit at the trench is the same as the current-day trench section (this assumption is also used for the reconstruction, as discussed in section 3) [e.g., *Bekins and Dreiss, 1992*]. Under these assumptions, the residence time of sediment in each region

is given by the solid area divided by the delivery rate of solids at the trench:

$$t = \frac{(1 - \gamma)A}{(1 - \gamma_0)H_0v_p}, \quad (2)$$

where  $\gamma$  and  $A$  are the porosity and area of the strata in a given region (e.g., PTZ, TS1, TS2),  $\gamma_0$  is the initial porosity at the trench reference location,  $H_0$  is the thickness of the section at the reference location, and  $v_p$  is the plate convergence rate. The dewatering flux ( $Q$ ) is then obtained by dividing the change in water content between regions by the residence time:

$$Q_n = \frac{(e_{n-1} - e_n)(1 - \gamma_{n-1})A_{n-1}}{t}, \quad (3)$$

where  $e$  is void ratio, the subscript  $n$  refers to the zone of interest, and  $(n-1)$  to the adjacent trenchward zone. The dewatering flux is expressed in units of  $\text{Vol}_{\text{H}_2\text{O}}/t$  per km along strike, and reflects the rate at which water is expelled due to consolidation as sediments are progressively incorporated into more arcward thrust slices.

[20] The computed dewatering rates are largest in the trench sediments, and in the outermost ~2–4 km of the accretionary wedge. Our results show that  $5 \text{ km}^3/\text{Ma}$   $\text{H}_2\text{O}$  (per km along strike) are expelled

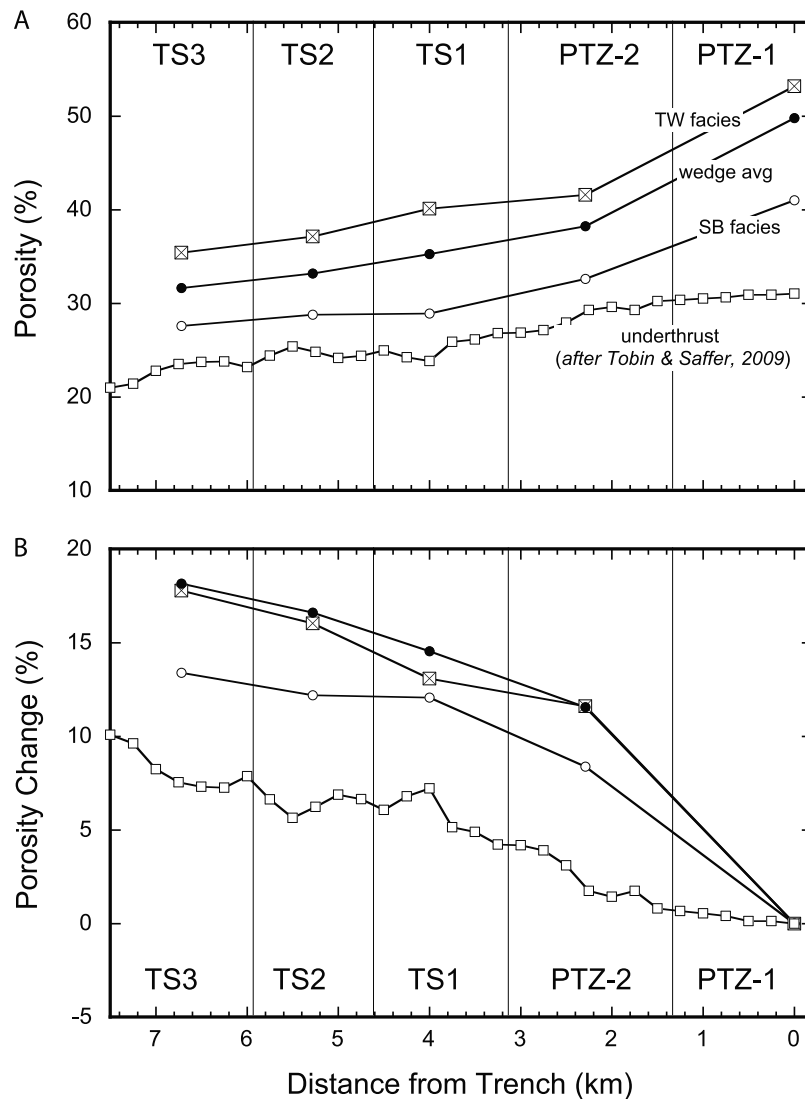


**Figure 8.** (a) Porosity and (b) change in porosity with distance into the subduction zone, for the trench wedge facies sediments (TW; boxes with crosses), accreted Shikoku Basin facies sediment (SB; open circles), and averaged values for the accreted sediment (closed circles), and underthrusting section (open boxes). Sign convention for porosity change in Figure 8b is that positive values indicate porosity loss. Although the underthrust section is undercompacted relative to the sediments immediately above [Moore *et al.*, 2001], it is not evident as plotted because the porosities reported for the Shikoku Basin facies are averaged over the lower several hundred meters of the accretionary wedge.

from the trench sediment between the trench and 2 km arcward, and  $6.75 \text{ km}^3/\text{Ma}$  between the trench and 6.5 km, whereas the accreted hemipelagic Shikoku Basin sediment releases  $1.7 \text{ km}^3/\text{Ma}$  and  $2.6 \text{ km}^3/\text{Ma}$  by 2 km and 6.5 km from the trench, respectively (Figure 9). When normalized by the volume of sediments undergoing dewatering, the fluid source terms (units of  $\text{Vol}_{\text{H}_2\text{O}}/\text{Vol}_{\text{sed}}$  per s) range from  $1.1 \times 10^{-14} \text{ s}^{-1}$  to  $1.2 \times 10^{-13} \text{ s}^{-1}$ , and are in good agreement with those computed in numerical modeling studies of the Muroto transect [Bekins and Dreiss, 1992; Saffer and Bekins,

1998]. For comparison, the underthrust Shikoku Basin section yields  $<0.4 \text{ km}^3/\text{Ma}$   $\text{H}_2\text{O}$  in the outer 2 km, and  $\sim 1.3 \text{ km}^3/\text{Ma}$  in the outer 6.5 km.

[21] The dewatering rates along the Muroto transect are similar, though slightly higher than those reported for the eastern Alaska margin [von Huene *et al.*, 1998] and along the Barbados margin [Screaton *et al.*, 1990], and slightly lower than those reported for sediments underthrust at the Costa Rican margin [Saffer, 2003](Figure 9). Normalized dewatering rates for the Peru margin range

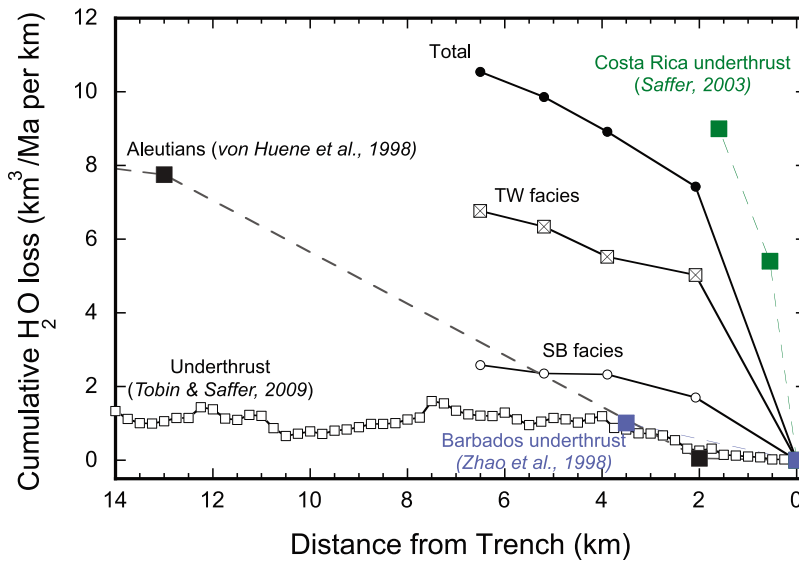


**Figure 9.** Cumulative dewatering as a function of distance from the trench, with the same legend as in Figure 8. For comparison, dewatering rates reported for the Alaska margin (gray squares), Costa Rican margin (green squares), and underthrusting sediment at the Barbados margin (blue squares) are also shown.

from  $3 \times 10^{-17}$  to  $3 \times 10^{-13}$  [Kukowski and Pecher, 1999]. The rates of fluid loss from the underthrusting section are comparable for the Muroto transect and the northern Barbados margin [Zhao *et al.*, 1998].

[22] The differences in dewatering fluxes between units along our transect, and between margins, can be explained by four primary factors: (1) initial sediment thickness, where larger sediment thickness leads to higher dewatering fluxes, (2) initial porosity, where higher initial porosity results in larger total pore volume and higher compressibility, both leading to higher dewatering rates, (3) plate convergence rate, which controls burial and tectonic loading rate, and (4) permeability, which governs the rate of fluid expulsion (as manifested in observed porosity loss) in response to loading. For example, the trench sediments in our study area are thicker than the accreted and underthrust Shikoku Basin sediment sections, and thicker than the underthrusting section at Barbados, leading to higher overall volumes of water expulsion (Figures 3–4 and 9). In addition, the initial porosity, and thus compressibility, of the trench sediments is higher than that of the Shikoku Basin sediment or the underthrust section at Barbados, owing to their shallower burial state at the trench. This leads to higher rates of compaction early in the loading history, as documented by the rapid porosity loss within the trench sediments in the outer few km of

the accretionary wedge (Figures 7–8). The trench sediments also contain abundant silty and sandy turbidites that should allow for efficient drainage and dewatering in comparison to the uniformly clay-rich Shikoku Basin facies or underthrust pelagic claystones at Barbados [e.g., Moore *et al.*, 2001; Steurer and Underwood, 2003]. At Costa Rica, the sediment section is only ~380 m thick, but the convergence rate of 88 km/Ma is higher than that at Nankai or Barbados (29 km/Ma), and the entire sediment column is highly porous, compressible, and permeable [e.g., Saffer, 2003], leading to efficient dewatering and rapid fluid expulsion there. Overall, our analysis is consistent with observations from several other well-studied margins, and provides additional insights into the interplay between sediment thickness, permeability, and plate convergence rate in controlling porosity loss and dewatering fluxes.

## 5. Conclusions

[23] Our analysis of the Muroto transect outer wedge toe focused on structural restoration through the contribution of tectonic area change in cross-section analyses, quantification of sediment compaction as a major contributor to total horizontal strain, and estimation of dewatering fluxes based on rates of porosity reduction. Our results reveal that ~60–75% of the total horizontal shortening of

sediment within the outer wedge toe is accommodated by consolidation and porosity loss during accretion in the northeast region of the Muroto transect. We show that significant distributed deformation occurs within sediments during the initial stages of accretion, resulting in a total horizontal shortening of ~40% within the first three thrust sheets of the wedge. The corresponding rates of dewatering are highest in the outermost ~2–4 km of the accretionary wedge and within the trench sediments, and decrease systematically with distance landward. This study highlights the importance of considering distributed compressive strain in structural restorations for any setting where deformation occurs in young sediments, including fold and thrust systems and accretionary wedges. Our analysis also provides quantitative estimates of both the amount of shortening due to porosity loss and dewatering fluxes.

## Acknowledgments

[24] B. Ratliff read a version of the manuscript and provided numerous insightful comments and suggestions, as well as training in section balancing. We thank him and Geo-Logic Systems (now Landmark/Halliburton) for the use of LithoTect™ software. We thank K. Wang and J. Morgan for many helpful discussions. Reviews of earlier drafts by T. Byrne and N. Bangs helped to clarify the presentation. The final version was significantly improved by reviews from the Associate Editor and reviewers. This research was supported by grants from the National Science Foundation and SOEST contribution 8111.

## References

- Ando, M. (1975), Source mechanisms and tectonic significance of historical earthquakes along the Nankai Trough, Japan, *Tectonophysics*, *27*, 119–140, doi:10.1016/0040-1951(75)90102-X.
- Aoki, Y., T. Tamano, and S. Kato (1982), Detailed structure of the Nankai Trough from migrated seismic sections, in *Studies in Continental Margin Geology*, edited by J. S. Watkins and C. L. Drake, *AAPG Mem.*, *34*, 309–322.
- Aoki, Y., H. Kinoshita, and H. Kagami (1986), Evidence of a low-velocity layer beneath the accretionary prism of the Nankai Trough: Inferences from a synthetic sonic log, *Initial Rep. Deep Sea Drill. Proj.*, *87*, 727–735.
- Bally, A. W., P. L. Gordy, and G. A. Stewart (1966), Structure, seismic data, and orogenic evolution of the southern Canadian Rocky Mountains, *Bull. Can. Pet. Geol.*, *14*, 337–381.
- Bangs, N. L., T. H. Shipley, S. P. S. Gulick, G. F. Moore, S. Kuromoto, and Y. Nakamura (2004), Evolution of the Nankai Trough décollement from the trench into the seismogenic zone: Inferences from three-dimensional seismic reflection imaging, *Geology*, *32*, 273–276, doi:10.1130/G20211.2.
- Bekins, B. A., and S. J. Dreiss (1992), A simplified analysis of parameters controlling dewatering in accretionary prisms, *Earth Planet. Sci. Lett.*, *109*, 275–287, doi:10.1016/0012-821X(92)90092-A.
- Bekins, B. A., and E. J. Screaton (2007), Pore pressure and fluid flow in the northern Barbados accretionary complex: A synthesis, in *The Seismogenic Zone of Subduction Thrust Faults*, edited by T. H. Dixon and J. C. Moore, pp. 148–170, Columbia Univ. Press, New York.
- Bray, C. J., and D. E. Karig (1985), Porosity of sediments in accretionary prisms and some implications for dewatering processes, *J. Geophys. Res.*, *90*, 768–778, doi:10.1029/JB090iB01p00768.
- Costa Pisani, P., M. Reshef, and G. Moore (2005), Targeted 3-D prestack depth imaging at Legs 190–196 ODP drill sites (Nankai Trough, Japan), *Geophys. Res. Lett.*, *32*, L20309, doi:10.1029/2005GL024191.
- Dahlstrom, C. D. A. (1969), Balanced cross sections, *Can. J. Earth Sci.*, *6*, 743–757.
- Davison, I. (1986), Listric normal fault profiles: Calculation using bed-length balance and fault displacement, *J. Struct. Geol.*, *8*, 209–210, doi:10.1016/0191-8141(86)90112-4.
- Gulick, S. P., N. L. Bangs, T. H. Shipley, Y. Nakamura, G. Moore, and S. Kuramoto (2004), Three-dimensional architecture of the Nankai accretionary prism's imbricate thrust zone off Cape Muroto, Japan: Prism reconstruction via an echelon thrust propagation, *J. Geophys. Res.*, *109*, B02105, doi:10.1029/2003JB002654.
- Henry, P., L. Jouniaux, E. J. Screaton, S. Hunze, and D. M. Saffer (2003), Anisotropy of electrical conductivity record of initial strain at the toe of the Nankai accretionary wedge, *J. Geophys. Res.*, *108*(B9), 2407, doi:10.1029/2002JB002287.
- Hyndman, R. D., G. F. Moore, and K. Moran (1993), Velocity porosity and pore-fluid loss from the Nankai subduction zone accretionary prism, *Proc. Ocean Drill. Program Sci. Results*, 211–220.
- Kimura, G., Y. Kitamura, Y. Hashimoto, A. Yamaguchi, T. Shibata, K. Ujiie, and S. Y. Okamoto (2007), Transition of accretionary wedge structures around the up-dip limit of the seismogenic subduction zone, *Earth Planet. Sci. Lett.*, *255*(3–4), 471–484, doi:10.1016/j.epsl.2007.01.005.
- Kodaira, S., N. Takahashi, J. O. Park, K. Mochizuki, M. Shinohara, and S. Kimura (2000), Western Nankai Trough seismogenic zone: Results from a wide-angle ocean bottom seismic survey, *J. Geophys. Res.*, *105*, 5887–5905, doi:10.1029/1999JB900394.
- Kopp, H., and N. Kukowski (2003), Backstop geometry and accretionary mechanics of the Sunda margin, *Tectonics*, *22*(6), 1072, doi:10.1029/2002TC001420.
- Kukowski, N., and I. Pecher (1999), Thermo-hydraulics of the Peruvian accretionary complex at 12°S, *J. Geodyn.*, *27*, 373–402, doi:10.1016/S0264-3707(98)00009-X.
- Leggett, J. K., Y. Aoki, and T. Toba (1985), Transition from frontal accretion to underplating in part of the Nankai Trough accretionary complex off Shikoku (SW Japan) and extensional features on the lower trench slope, *Mar. Pet. Geol.*, *2*, 131–141, doi:10.1016/0264-8172(85)90003-0.
- Le Pichon, X., P. Henry, and S. Lallemand (1990), Water flow in the Barbados accretionary complex, *J. Geophys. Res.*, *95*, 8945–8967, doi:10.1029/JB095iB06p08945.
- Mikada, H., et al. (2002), *Proceedings of the Ocean Drilling Program, Initial Reports* [CD-ROM], vol. 196, Ocean Drilling Program, College Station, Tex.

- Miyazaki, S., and K. Heki (2001), Crustal velocity field of southwest Japan: Subduction and arc-arc collision, *J. Geophys. Res.*, *106*, 4305–4326, doi:10.1029/2000JB900312.
- Moore, G. F., T. H. Shipley, P. L. Stoffa, D. E. Karig, A. Taira, S. Kuramoto, H. Tokuyama, and K. Suyehiro (1990), Structure of the Nankai Trough accretionary zone from multichannel seismic reflection data, *J. Geophys. Res.*, *95*, 8753–8765, doi:10.1029/JB095iB06p08753.
- Moore, G. F., D. E. Karig, T. H. Shipley, A. Taira, P. L. Stoffa, and W. T. Wood (1991), Structural framework of the ODP Leg 131 area, Nankai Trough, *Ocean Drill. Program Initial Rep.*, *131*, 15–20.
- Moore, G. F., et al. (1999), Structural setting of the Leg 190 Muroto transect, *Ocean Drill. Program Initial Rep.*, *190*, 1–14. doi:10.2973/odp.proc.ir.190.102.2001.
- Moore, G. F., et al. (2001), New insights into deformation and fluid flow processes in the Nankai Trough accretionary prism: Results of Ocean Drilling Program Leg 190, *Geochem. Geophys. Geosyst.*, *2*, 1058, doi:10.1029/2001GC000166.
- Moore, J. C., et al. (1998), Consolidation patterns during initiation and evolution of a plate-boundary decollement zone: Northern Barbados accretionary prism, *Geology*, *26*(9), 811–814, doi:10.1130/0091-7613(1998)026<0811:CPDIAE>2.3.CO;2.
- Morgan, J. K., and D. E. Karig (1995), Kinematics and a balanced and restored cross-section across the toe of the eastern Nankai accretionary prism, *J. Struct. Geol.*, *17*(1), 31–45, doi:10.1016/0191-8141(94)E0031-S.
- Morgan, J. K., E. B. Ramsey, and M. V. S. Ask (2007), Deformation and mechanical strength of sediments at the Nankai subduction zone: Implications for prism evolution and décollement initiation and propagation, in *The Seismogenic Zone of Subduction Thrust Faults*, edited by T. H. Dixon and J. C. Moore, pp. 210–256, Columbia Univ. Press, New York.
- Ohmori, K., A. Taira, H. Tokuyama, A. Sakaguchi, M. Okamura, and A. Aihara (1997), Paleothermal structure of the Shimanto accretionary prism, Shikoku, Japan; role of an out-of-sequence thrust, *Geology*, *25*, 327–330, doi:10.1130/0091-7613(1997)025<0327:PSOTSA>2.3.CO;2.
- Park, J. O., T. Tsuru, Y. Kaneda, and Y. Kono (1999), A subducting seamount beneath the Nankai accretionary prism off Shikoku, southwestern Japan, *Geophys. Res. Lett.*, *26*, 931–934, doi:10.1029/1999GL900134.
- Park, J. O., S. Miura, Y. Kaneda, Y. Kono, T. Tsuru, S. Kodaira, and A. Nakanishi (2000), Out-of-sequence thrust faults developed in the coseismic slip zone of the 1946 Nankai earthquake ( $M_w = 8.2$ ) off Shikoku, southwest Japan, *Geophys. Res. Lett.*, *27*, 1033–1036, doi:10.1029/1999GL008443.
- Park, J. O., S. Kodaira, A. Nakanishi, S. Miura, Y. Kaneda, T. Tsuru, N. Takahashi, and T. Horii (2002), A deep strong reflector in the Nankai accretionary wedge from multichannel seismic data: Implications for underplating and interseismic shear stress release, *J. Geophys. Res.*, *107*(B4), 2061, doi:10.1029/2001JB000262.
- Saffer, D. M. (2003), Pore pressure development and progressive dewatering in underthrust sediments at the Costa Rican subduction margin: Comparison with Northern Barbados and Nankai, *J. Geophys. Res.*, *108*(B5), 2261, doi:10.1029/2002JB001787.
- Saffer, D. M., and B. A. Bekins (1998), Episodic fluid flow in the Nankai accretionary complex: Timescale, geochemistry, flow rates, and fluid budget, *J. Geophys. Res.*, *103*, 30,351–30,370, doi:10.1029/98JB01983.
- Saffer, D. M., and B. A. Bekins (2002), Hydrologic controls on the morphology and mechanics of accretionary wedges, *Geology*, *30*, 271–274, doi:10.1130/0091-7613(2002)030<0271:HCOTMA>2.0.CO;2.
- Screaton, E. J., D. R. Wuthrich, and S. J. Dreiss (1990), Permeabilities, fluid pressures, and flow rates in the Barbados Ridge Complex, *J. Geophys. Res.*, *95*, 8997–9007, doi:10.1029/JB095iB06p08997.
- Screaton, E. J., et al. (2002), Porosity loss within the underthrust sediments of the Nankai accretionary complex; implications for overpressures, *Geology*, *30*, 19–22, doi:10.1130/0091-7613(2002)030<0019:PLWTUS>2.0.CO;2.
- Seno, T., S. Stein, and A. E. Gripp (1993), A model for the motion of the Philippine Sea plate consistent with NUVEL-1 and geological data, *J. Geophys. Res.*, *98*, 17,941–17,948, doi:10.1029/93JB00782.
- Shaw, J. H., C. D. Connors, and J. Suppe (Eds.) (2005), *Seismic Interpretation of Contractional Fault-Related Folds*, AAPG Stud. Geol., vol. 53, 156 pp., Am. Assoc. of Pet. Geol., Tulsa, Okla.
- Shipley, T. H., G. F. Moore, N. Bangs, J. C. Moore, and P. L. Stoffa (1994), Seismically inferred dilatancy distribution, northern Barbados Ridge decollement: Implications for fluid migration and fault strength, *Geology*, *22*, 411–414, doi:10.1130/0091-7613(1994)022<0411:SIDDNB>2.3.CO;2.
- Shipley, T., et al. (1995), *Proceedings of the Ocean Drilling Program, Initial Reports*, vol. 196, 301 pp., Ocean Drill. Program, College Station, Tex.
- Steurer, J. F., and M. B. Underwood (2003), Clay mineralogy of mudstones from the Nankai Trough reference Sites 1173 and 1177 and frontal accretionary prism Site 1174 [online], *Proc. Ocean Drill. Program Sci. Results, 190/196*. [Available at <http://www-odp.tamu.edu/publications/190196SR/211/211.htm>.]
- Suppe, J. (1983), Geometry and kinematics of fault-bend folding, *Am. J. Sci.*, *283*, 684–721, doi:10.2475/ajs.283.7.684.
- Taira, A. (2001), Tectonic evolution of the Japanese Island Arc System, *Annu. Rev. Earth Planet. Sci.*, *29*, 109–134, doi:10.1146/annurev.earth.29.1.109.
- Taira, A., J. Katto, M. Tashiro, M. Okamura, and K. Kodama (1988), The Shimanto Belt in Shikoku Japan: Evolution of a Cretaceous to Miocene accretionary prism, *Mod. Geol.*, *12*, 5–46.
- Taira, A., et al. (1991), *Proceedings of the Ocean Drilling Program, Initial Reports*, vol. 131, 301 pp., Ocean Drill. Program, College Station, Tex.
- Tobin, H. J., and D. M. Saffer (2009), Elevated fluid pressure and extreme mechanical weakness of a plate boundary thrust, Nankai Trough subduction zone, *Geology*, *37*, 679–682, doi:10.1130/G25752A.1.
- von Huene, R., and D. Klaeschen (1999), Opposing gradients of permanent strain in the aseismic zone and elastic strain across the seismogenic zone of the Kodiak shelf and slope, Alaska, *Tectonics*, *18*, 248–262, doi:10.1029/1998TC900022.
- von Huene, R., D. Klaeschen, M.-A. Gutscher, and J. Fruehn (1998), Mass and fluid flux during accretion at the Alaskan margin, *Geol. Soc. Am. Bull.*, *110*, 468–482, doi:10.1130/0016-7606(1998)110<0468:MAFFDA>2.3.CO;2.
- Westbrook, G. K., J. W. Ladd, and N. L. Bangs (1988), Cross section of an accretionary wedge: Barbados Ridge complex, *Geology*, *16*, 631–635, doi:10.1130/0091-7613(1988)016<0631:CSOAAW>2.3.CO;2.



Westbrook, G. K., et al. (1994), *Proceedings of the Ocean Drilling Program, Initial Reports*, vol. 146 (Part 1), 611 pp., Ocean Drill. Program, College Station, Tex.

Woodward, N. B., S. E. Boyer, and J. Suppe (1985), An outline of balanced cross-sections: Notes from Geological Society of America short course on balanced sections, *Stud. Geol.*, 11, 2nd ed., 170 pp., Univ. of Tenn., Knoxville, Tenn.

Xiao, H., and J. Suppe (1993), Origin of rollover, *Am. Assoc. Pet. Geol. Bull.*, 76, 509–529.

Zhao, Z., G. F. Moore, and T. H. Shipley (1998), Deformation and dewatering of the subducting plate beneath the lower slope of the northern Barbados accretionary prism, *J. Geophys. Res.*, 103, 30,431–30,449, doi:10.1029/1998JB900012.